

The anatomical pathway from the mesodiencephalic junction to the inferior olive relays perioral sensory signals to the cerebellum in the mouse

Reika Kubo¹, Atsu Aiba² and Kouichi Hashimoto¹ 

¹Department of Neurophysiology, Graduate School of Biomedical and Health Sciences, Hiroshima University, 1-2-3 Kasumi, Minami-ku, Hiroshima 734-8551, Japan

²Laboratory of Animal Resources, Center for Disease Biology and Integrative Medicine, Graduate School of Medicine, The University of Tokyo, Tokyo 113-0033, Japan

Edited by: Ian Forsythe & Michisuke Yuzaki

Key points

- Perioral tactile signals are transmitted via the infraorbital nerve (ION) to trigeminal nuclei. Each cerebellar Purkinje cell (PC) receives this signal as complex spikes (CSs) via a climbing fibre (CF) emerging from the inferior olive (IO).
- The anatomical pathway from trigeminal nuclei to the IO is not clearly identified.
- In the present study, we examined candidate anatomical pathways for perioral sensory signalling by analysing CSs recorded from PCs in male mice by single unit recording.
- CS generation by ION stimulation was inhibited by injection of a GABA_A receptor agonist, muscimol, into the contralateral mesodiencephalic junction, which is referred to as the area parafascicularis prerubralis (PfPr). The number of CSs evoked by mechanical whisker stimulation was also decreased by contralateral PfPr inhibition.
- These results suggest the existence of a sensory signalling pathway to the IO via the PfPr in mice.

Abstract Perioral tactile signals are transmitted via the infraorbital nerve (ION) to trigeminal nuclei. Each cerebellar Purkinje cell receives this signal as complex spikes (CSs) via a climbing fibre emerging from the inferior olive (IO). However, the anatomical pathway from the trigeminal nuclei to the IO is not clearly identified. In the present study, we recorded CSs from Purkinje cells in male mice by single unit recording, and examined the signal transduction pathway. CSs were evoked by electrical stimulation of the ipsilateral or contralateral ION with a latency of

Reika Kubo obtained her master's degree in Medical Science at Hiroshima University, Japan, in 2014. She is currently a PhD student in the Department of Neurophysiology at Hiroshima University. She studies neural circuits for the sensory signal transduction in the mammalian brain using electrophysiological techniques and optogenetics.



20–70 ms. CS generation by ipsilateral ION stimulation was inhibited by injection of a GABA_A receptor agonist, muscimol, into the contralateral mesodiencephalic junction, ranging from around the fasciculus retroflexus to the interstitial nucleus of Cajal, which is referred to as the area parafascicularis prerubralis (PfPr). CSs evoked by contralateral ION stimulation were also suppressed by muscimol injection into the PfPr, although the effective area was more restricted. Furthermore, CSs evoked by mechanical stimulation around the whisker region were suppressed by PfPr inhibition. We also found that the primary motor cortex plays a role to suppress this signalling pathway. These results indicate the existence of an anatomical pathway for conducting perioral sensory signals to the IO via the PfPr.

(Received 13 January 2018; accepted after revision 14 May 2018; first published online 29 May 2018)

Corresponding author K. Hashimoto: Department of Neurophysiology, Graduate School of Biomedical and Health Sciences, Hiroshima University, 1-2-3 Kasumi, Minami-ku, Hiroshima 734-8551, Japan. Email: hashik@hiroshima-u.ac.jp

Introduction

Tactile information is transmitted to the somatosensory cortex and processed to control motor functions. The rodent whisker system has been widely used to study sensorimotor integration in the brain (Bosman *et al.* 2011; Kleinfeld & Deschenes, 2011; Diamond & Arabzadeh, 2013; Feldmeyer *et al.* 2013; Petersen, 2014). In addition to transduction to the cerebral cortex, tactile information is transmitted to the cerebellum via climbing fibres (CFs) and mossy fibres (Brown & Bower, 2001; Lang, 2001; Bosman *et al.* 2010). CFs are axons emerging from the contralateral inferior olive (IO), and they form strong synapses on cerebellar Purkinje cells (PCs) (Cintas *et al.* 1980; Paxinos, 2004; Sugihara *et al.* 2007). Each PC receives only one CF projection, and its activation evokes strong depolarization in PCs, termed complex spikes (CSs) (Brown & Bower, 2001; Lang, 2001; Bosman *et al.* 2010). Therefore, CS generation in a recorded PC reflects activation of the presynaptic IO neuron.

In the cerebellar system, Crus I and Crus II receive perioral tactile information from the contralateral IO in highly organized patterns (Huerta *et al.* 1983; Buisseret-Delmas & Angaut, 1993; Brown & Bower, 2001; Sugihara *et al.* 2007). However, the anatomical pathway for perioral sensory signals to the IO remains controversial. Facial tactile signals are mainly transmitted by the trigeminal nerve, which has three major branches (ophthalmic, maxillary and mandibular nerves). Whiskers and sinus hairs on the snout are innervated by the infraorbital nerve (ION), a branch of the maxillary nerve, in the rodent. Perioral tactile signals are initially transmitted through the ION to trigeminal nuclei. The IO receives direct anatomical inputs from bilateral, but principally contralateral, spinal trigeminal nucleus oral, interpolar and caudal parts (SpVo, SpVi and SpVc, respectively) (Huerta *et al.* 1983; Swenson & Castro, 1983; De Zeeuw *et al.* 1996; Molinari *et al.* 1996; Yatim *et al.* 1996). If this pathway is activated for conducting sensory signals, perioral stimulation ipsilateral to the recorded PCs would be more

effective in evoking CSs than contralateral stimulation. However, in previous studies, contralateral whisker or trigeminal nerve stimulation also effectively evoked CSs (Miles & Wiesendanger, 1975*a, b*; Armstrong & Drew, 1980; Mülle *et al.* 1987; Akaike, 1988; Thomson *et al.* 1989). Akaike (1988) reported that CS generation by contralateral whisker stimulation was blocked by suction removal of the superior colliculus ipsilateral to the recorded PCs. These lines of evidence suggest the existence of various signalling pathways for perioral sensory transduction to PCs.

Previous reports have demonstrated that stimulation of the sensorimotor cortex elicits CSs in rats and cats (Provini *et al.* 1968; Leicht *et al.* 1973; Miles & Wiesendanger, 1975*a*; Lang, 2001; Ackerley *et al.* 2006). Moreover, Armstrong & Drew (1980) reported that CS generation by electrical stimulation of the perioral area was strongly suppressed by mid-collicular decerebration in rats. Therefore, the cerebral cortex may be a candidate relay for tactile signal transduction to the PC via the IO. In addition, the IO also receives principally ipsilateral inputs from a broad area around the mesodiencephalic junction. Neurons projecting to the IO show a borderless distribution from around the fasciculus retroflexus (fr) in the thalamus to the interstitial nucleus of Cajal (INC) and the nucleus of Darkschewitsch (ND) in the midbrain (Brown *et al.* 1977; Cintas *et al.* 1980; Carlton *et al.* 1982; Swenson & Castro, 1983; Bentivoglio & Molinari, 1984; De Zeeuw *et al.* 1990; Paxinos, 2004). In previous reports, this broad area was referred to as the 'area parafascicularis prerubralis' (PfPr) (Carlton *et al.* 1982; Paxinos, 2004). Because trigeminal nuclei are known to project to the mesencephalic reticular formation, ND and parafascicular nucleus (PF) involved in this area (Veazey & Severin, 1982; Onodera & Hicks, 1995; Krout *et al.* 2002), the PfPr is also a candidate relay for the tactile signalling pathway to the IO (Akaike, 1988).

In the present study, we examined the signalling pathway for CS generation by electrical stimulation of the ION. Stimulation of the right ION (r-ION) ipsilateral to the recorded PC in the right lateral Crus II evoked CSs in PCs with a latency of 20–70 ms. Suppression of neuronal

activity around the primary motor cortex (MI) did not suppress, but rather enhanced, CS generation by r-ION stimulations. By contrast, local injections of muscimol into the left PfPr (l-PfPr) contralateral to the recorded PCs effectively blocked CSs. CSs evoked by mechanical stimulation to the perioral area were also suppressed by muscimol injections into the l-PfPr. These data suggest the existence of an anatomical pathway for perioral sensory transduction through the PfPr in mice.

Methods

Ethical approval

All animal experiments were performed in accordance with guidelines from the Animal Research Committee (#A16-137, #M-P14-117) and the biosafety committee for living modified organisms (#28-223, #47) of Hiroshima University and The University of Tokyo. The investigators understand the ethical principles under which the journal operates, and our work complies with the animal ethics checklist. Male C57BL/6J, ArchT-EGFP or Emx1-Cre mice (approximately 25 g) at approximately post-natal day 60 were used in all experiments. The total number of animals used for experiments was 81 for C57BL/6J and nine for ArchT-EGFP/Emx1-Cre mice. C57BL/6J mice were obtained from CREA Japan and Charles River Laboratories Japan. ArchT-EGFP mice were obtained from the Jackson Laboratory (#021188, Jackson Laboratory, <https://www.jax.org/strain/021188>). Details of the generation of Emx1-Cre mice were previously described (Kassai *et al.* 2008). We maintained all mice in specific pathogen free facilities (SPF) on a reverse 12 h light/dark cycle (lights off at 20:00) with free access to food and water.

Single unit recording

Animals were anaesthetized by intraperitoneal injection of a mixture of ketamine (100 mg/kg; Daiichi Sankyo, Tokyo, Japan) and xylazine (10 mg/kg; Bayer Yakuin, Osaka, Japan). The depth of anaesthesia was monitored by vibrissae movements. Under deep anaesthesia, the mystacial pad only on the stimulated side was moved by ION stimulations, without sporadic movements. All CSs except for those in Fig. 5 were recorded in this condition. When sporadic whisker movements were detected or both sides of mystacial pads were simultaneously moved by stimulations to one side of the ION, a mixture of ketamine (13 mg/ml) and xylazine (1.3 mg/ml) was administered from a cannula with a needle inserted into hind limb muscles. This anaesthetic mixture was administered approximately 40 μ l per injection, until the contralateral mystacial pad movement stopped. The

total supplemental volume of the mixture did not exceed 200 μ l. Body temperature was maintained at $37 \pm 1^\circ\text{C}$ using a heating pad (FHC, Bowdoin, ME, USA). After reaching a surgical level of anaesthesia, the animal's head was fixed in a stereotaxic apparatus (Narishige, Tokyo, Japan), an incision was made in the skin, and the skull over the right cerebellum was exposed by removing muscles and connective tissues. Lidocaine gel (AstraZeneca, Cambridge, UK) was applied to the skin incision. A craniotomy (1–2 mm in diameter) was performed using a micro-drill (Nakanishi, Tokyo, Japan) at approximately 3.5 mm lateral from the midline on the occipital bone over a right cerebellar folium (Crus II). The craniotomy was then filled with 1.5% low-melting-point agarose dissolved in Hepes-buffered saline containing (in mM): 150 NaCl, 2.5 KCl, 10 Hepes, 2 CaCl₂, 1 MgCl₂ (pH 7.4, adjusted with NaOH).

Single units were recorded from PCs in the right Crus II with a Multiclamp 700B or an Axopatch 200B amplifier (Molecular Devices, San Jose, CA, USA). Glass microelectrodes were filled with Hepes-buffered saline, and the resistance of the filled electrodes was 4–9 M Ω . The pipette was advanced by 2 μ m steps using a stepping micromanipulator (Narishige). PCs were identified by the generation of simple and complex spikes. Electrophysiological data were recorded in the current clamp mode, low-pass filtered at 10 kHz and digitized at 20 kHz, and acquired with Axograph X software (Axograph Scientific, Sydney, Australia). Data were analysed with Excel (Microsoft, Redmond, WA, USA) or OriginPro (OriginLab, Northampton, MA, USA). Data were high-pass filtered at 300 Hz to remove field potentials after recording. Peri-stimulus spike density functions (SDFs) were calculated by convolving the registered neuronal spikes with a Gaussian function (σ value = 2 ms).

To perform CS recording in the lightly anaesthetized state, mice were allowed to recover from anaesthesia after surgery for the single unit recording, and the CS was then recorded during the lightly anaesthetized state. In this condition, leg or body movements were not observed, but the rate of sporadic whiskering was increased. In addition, stimulation of one side of the ION caused movements of both sides of mystacial pads in the lightly anaesthetized state, suggesting activation of more complex pathways that were suppressed under deep anaesthesia. When leg or body movements became frequent, 20 μ l of a mixture of ketamine and xylazine, about a half dose for maintaining deep anaesthesia, was administered.

For ION stimulation, both sides of the ION were exposed under a stereoscopic microscope (M60; Leica, Wetzlar, Germany). The incision was made below the eye at 1 mm caudal to the mystacial pad. The muscles were dissected to expose the ION, and cathode and anode of the bipolar tungsten electrodes (interpolated distance = 2 mm) were placed on the afferent and efferent sides of the

exposed ION, respectively. Stimuli (duration, 0.3 ms; amplitude, 1–4 mA) were applied every 3 s. The incidence of CSs showed a trend towards an increase with stimulus intensity but became saturated or decreased at higher intensity. Stimulus strength was adjusted to evoke CSs at the highest incidence. For mechanical stimulation of the perioral area, air pressure (0.34 MPa, 5 ms) was applied using a Picospritzer III (Parker, Mayfield Heights, OH, USA). The air pressure was delivered by a polyethylene tube (1 mm diameter) connected to a glass capillary (0.86 mm diameter) that was placed approximately 3 mm above the right or left whisker area.

At the end of experiments, mice were deeply anaesthetized by an overdose of the ketamine/xylazine mixture used for anaesthetic induction, and the brains fixed by transcardial perfusion with 4% paraformaldehyde (Nakalai Tesque, Kyoto, Japan) in 0.1 M phosphate buffer (PB) (pH 7.5). Coronal sections (100 μm in thickness) were cut with a microslicer (Dosaka, Kyoto, Japan) for histological analysis. In some experiments, the cerebellar cortex was immunostained by aldolase C antibody (Cat. No. AldolaseC-Rb-Af1390, RRID:AB_2571658; Frontier Institute, Japan). Brains were removed, postfixed in the same fixative at 4°C overnight, immersed in 30% sucrose in 0.1 M sodium phosphate buffer (PBS) (pH 7.4), embedded in optimal cutting temperature compound (Sakura Finetek, Tokyo, Japan) and then frozen. Coronal sections (40 μm thick) were cut with a cryostat (Leica). The slices were incubated in 10% normal donkey serum, then in primary antibodies overnight at 4°C. After incubation with the primary antibodies, sections were washed and then incubated in AlexaFluor 488- (1:1000; Thermo Fisher Scientific, Waltham, MA, USA) conjugated species-specific secondary antibodies for 2 h at room temperature.

Muscimol injections

For muscimol injection into the MI or primary somatosensory cortex (SI), the skull over the bilateral cerebral cortex was exposed and two craniotomies (approximately 2 mm in diameter) were performed under anaesthesia. Muscimol (50 mM; Tocris, Bristol, UK) and Chicago Sky Blue 6B (20 mg/ml; Sigma-Aldrich, St Louis, MO, USA) were dissolved in Hepes-buffered saline. The muscimol solution (70 nl per injection) was pressure-injected into the centre of the cortical layer (around layer IV) on both sides of the cortex using a nano-injector equipped with a glass microelectrode (Nanoject II; Drummond, Broomall, PA, USA), at a flow rate of 23 nl/s. Injections into the MI were performed at 1.0–1.5 mm anterior and 0.7–1.5 mm lateral to bregma. SI injection sites were at 0.7–1.2 mm posterior and 2.5–3.0 mm lateral to bregma.

For injection into the mesodiencephalic junction, a craniotomy was performed over the left cerebral cortex. Injections were performed from the dorso-rostral side into the left PfPr with the injection electrode tilted 30° from the perpendicular line on the sagittal plane. A mixture of muscimol and Chicago Sky Blue 6B used for cortical suppression (70 nl, flow rate of 23 nl/s) was injected at –0.4 to 2.7 mm rostral and 2.1–3.8 mm dorsal to the interaural line, and 0.4–1.5 mm lateral to the midline. In some experiments (see Fig. 7), a glass microelectrode filled with Hepes-buffered saline was inserted into the PfPr for electrical stimulation.

After recording, mice were deeply anaesthetized by an overdose administration of the ketamine/xylazine mixture, and then fixed by transcardial perfusion with 4% paraformaldehyde (Nakalai Tesque) in 0.1 M PB (pH 7.5). Coronal sections (100 μm thick) were cut with a microslicer, and then counterstained using cresyl violet solution (MUTO, Tokyo, Japan). Injection sites were confirmed by Chicago Sky Blue 6B staining.

Optogenetic inactivation of cortical pyramidal neurons

Mutant mice in which cortical pyramidal neurons expressed ArchT were anaesthetized with a mixture of ketamine (100 mg/kg) and xylazine (10 mg/kg). A craniotomy over the left MI or SI was performed, but the dura was left intact. A 3 × 4 square grid (pitch = 1 mm, bar width = 0.05 mm) for the SI, or a 3 × 3 square grid for the MI, was placed on the dura as shown in Fig. 2C and E, respectively. First, 100 control CS recordings by r-ION stimulation without light were performed. Thereafter, a plastic optical fibre (0.5 mm diameter) was placed in one of the grid columns on the dura using a micromanipulator (Narishige). Yellow light (575 nm, 52 mW/mm²) was generated by laser diodes (Lumencor, Beaverton, OR, USA) and applied through the optical fibre for 200 ms starting at 100 ms before the onset of each ION stimulation (100 times). After recording from a grid column, the optical fibre was systematically moved to other columns. In some experiments with a large cortical craniotomy, CSs showed a longer average latency than those recorded without the craniotomy. PCs were omitted from analyses if the average control CS latency was longer than the mean + 1.5 SD of that without cortical craniotomy. In some experiments, the recording electrode was inserted into layers V–VI to test suppression by laser exposure (Fig. 2A, B).

Anterograde and retrograde tracer injections

Under anaesthesia induced by a mixture of ketamine (100 mg/kg) and xylazine (10 mg/kg), a glass pipette

filled with 2–3 μl of 10% biotinylated dextran amine (BDA) solution (10,000 MW; Invitrogen, Carlsbad, CA, USA) in PBS (pH 7.4) or Fluoro-Gold (FG; Wako, Osaka, Japan) dissolved in saline was inserted stereotaxically into the caudal part of the left PfPr (0.6–0.9 mm rostral and 2.2–2.7 mm dorsal to the interaural line, 0.4–0.7 mm lateral to the midline). BDA (70 nl) or FG (15 nl) was pressure-injected using a nanoinjector equipped with a glass microelectrode (Nanoject II), at a flow rate of 23 nl/s. After tracer injection, the wound was stitched with silk suture (Φ 0.4–0.5 mm; Natsume Seisakusho, Tokyo, Japan) and disinfected with 70% ethanol. Mice were moved to the cage with a heating lamp, and anaesthetic depth was checked approximately every 15 min. After recovery from anaesthesia, mice were moved to their home cage with free access to food and water.

After 4 days of recovery, mice were deeply anaesthetized with an overdose administration of the ketamine/xylazine mixture, and then fixed by transcardial perfusion with 4% paraformaldehyde in 0.1 M PB (pH 7.0–7.5). After overnight post-fixation in the same fixative, brains were immersed in 30% sucrose in 0.1 M PBS (pH 7.4), and then embedded in optimal cutting temperature compound (Sakura Finetek) and frozen. Coronal sections (40 μm thick) were cut with a cryostat (Leica). Slices were counterstained with NeuroTrace 500/525 Green Fluorescent Nissl Stain (Thermo Fisher Scientific). BDA was visualized with Alexa 568-conjugated streptavidin. Images were taken with a confocal laser scanning microscope (LSM 700; Zeiss, Oberkochen, Germany) or a fluorescence microscope (BZ-9000; Keyence, Osaka, Japan).

Statistics

For all experiments, mice were randomly allocated to experimental groups. In most experiments, CSs were recorded from only one PC in each mouse. Averaged data in the text are presented as the mean \pm SD. Data in the figures are presented as the mean \pm SEM. Statistical significance was assessed by two-sided paired *t*-tests or *t*-tests. Differences between groups were considered significant at $*P < 0.05$ and $**P < 0.01$. Statistical analyses were conducted with SigmaPlot 12.5 (RRID: SCR_010285, Systat Software, Chicago, IL, USA) or OriginPro (OriginLab).

Results

Complex spikes are evoked by ipsilateral or contralateral ION stimulation

Perioral tactile signals are initially transmitted through the ION to ipsilateral trigeminal nuclei. In the present study, we evoked CSs by electrical stimulation of the

ION to assess latencies of CSs accurately. All recordings (except for data shown in Fig. 5) were performed under anaesthesia to suppress spontaneous and unidentified sensory activation of PCs. The IO is known to receive direct anatomical inputs from the principally contralateral SpVs, and sends CFs to the contralateral cerebellum (Huerta *et al.* 1983; Swenson & Castro, 1983; De Zeeuw *et al.* 1996; Molinari *et al.* 1996; Yatim *et al.* 1996). If this pathway is activated for conduction of perioral sensory signals, ipsilateral ION stimulation would be more effective in evoking CSs than contralateral ION stimulation. However, the effectiveness of ipsilateral and contralateral perioral stimulation for CS generation differs in previous studies (Miles & Wiesendanger, 1975a; Cook & Wiesendanger, 1976; Armstrong & Drew, 1980; Mulle *et al.* 1987; Akaike, 1988; Thomson *et al.* 1989; Brown & Bower, 2001; Bosman *et al.* 2010) and depends, at least in part, on the location of the analysed PCs in the cerebellar cortex (Miles & Wiesendanger, 1975a, b). Therefore, we first checked the effectiveness of ipsilateral and contralateral ION stimulation to evoke CSs in our study.

All PCs were randomly recorded from the right lateral Crus II (see Methods). The r-ION stimulation generated CSs at latencies of 20–70 ms (39.1 ± 9.4 ms), with an incidence of 29.9 ± 16.3 spikes per 100 r-ION stimulations ($n = 44$ cells, $n = 39$ animals; Fig. 1A–C). The generation of CSs, even spontaneous ones, was transiently suppressed after 70 ms (Fig. 1B, C). The latency of CSs elicited up to 100 ms after r-ION stimulation was identical to that previously reported in rats (Mulle *et al.* 1987; Brown & Bower, 2001; Lang, 2001; Bosman *et al.* 2010). In the present study, we focused on the anatomical pathway for the CSs generated up to 100 ms after stimulation. After recording of CSs, we checked the location of nine out of 44 PCs in the right Crus II. The internal solution used for this experiment was supplemented with dextran Alexa fluor 568. The locations of the recorded PCs in immunostained aldolase C-positive or -negative stripes were detected by dextran Alexa fluor 568 (Fig. 1G). In the nine PCs, the latency of CSs (38.9 ± 6.6 ms; $n = 9$ cells, $n = 9$ animals) was not significantly different from that shown in Fig. 1. These nine PCs were distributed at relatively lateral areas of Crus II, which corresponds to 6+ (D1 zone, $n = 4$ cells, $n = 4$ animals) and 7+ (D2 zone, $n = 5$ cells, $n = 5$ animals) compartments (Sugihara & Shinoda, 2004).

Next, we examined whether stimulation of the left ION (l-ION) contralateral to the recorded PC evoked CSs. Stimulus intensity for the l-ION (2.0 ± 0.6 mA, $n = 44$ cells, $n = 39$ animals) was not significantly different from those of the r-ION (1.9 ± 0.5 mA, $n = 44$ cells, $n = 39$ animals; $P = 0.21$, *t*-test). Stimulation of the l-ION elicited CSs in all PCs in which CSs were evoked by r-ION stimulation. The averaged incidence of CSs was approximately 27 spikes per 100 stimulations ($27.0 \pm 16.9\%$, $n = 44$ cells, $n = 39$ animals), which was

not significantly different from that of r-ION stimulation ($P = 0.41$, t -test) (Fig. 1D–F). The latency of CSs evoked by l-ION stimulation (43.7 ± 7.9 ms, $n = 44$ cells, $n = 39$ animals) was significantly slower than that evoked by r-ION stimulation after pairwise comparison (** $P = 0.000015$, paired t -test), suggesting that signals from the l-ION conduct through a pathway partially different from that for r-ION (longer conduction length and/or involvement of axons with slower conduction velocity). However, the overall distribution of SDFs of r-

and l-ION stimulations almost overlapped at 20–70 ms (Fig. 1C, F), suggesting that the conduction length from the l-ION to the left IO (l-IO) was not markedly longer than that from the r-ION.

The somatosensory and motor cortices are not directly involved in signal transduction from the ION to PCs via the IO

Numerous reports have demonstrated that stimulation of the cerebral cortex elicits CSs (Provini *et al.* 1968; Leicht *et al.* 1973; Miles & Wiesendanger, 1975a; Lang, 2001; Ackerley *et al.* 2006). In addition, CS generation by stimulation of the perioral area is strongly suppressed by mid-collicular decerebration in rats (Armstrong & Drew, 1980). These data suggest that the cerebral cortex may be involved in the sensory signalling pathway to the IO. We tested this hypothesis by local inhibition of cortical activity. ArchT was expressed in pyramidal neurons in the cerebral cortex by crossing ArchT-EGFP mice that carry a Cre-mediated expression gene encoding ArchT-EGFP fusion protein, with *Emx-1* Cre mice that express Cre in layer II–III and V–VI pyramidal neurons (Kassai *et al.* 2008). In these mice, enhanced green fluorescent protein (EGFP) was strongly expressed in the entire cerebral cortex (Fig. 2A) (Iwasato *et al.* 2000; Kassai *et al.* 2008). We recorded multi-unit recordings from layers V–VI in the left SI and checked the suppression of firing activity evoked by r-ION stimulation by yellow light illumination (575 nm, 52 mW/mm²) delivered from a 500 μ m diameter optical fibre placed on the dura (Fig. 2A, B). Yellow light illumination of the left SI suppressed multiunit spikes evoked by r-ION stimulation by approximately 55% of control (number of spikes evoked by 100 r-ION stimulations: 220 ± 106.4 in control vs. 98 ± 69.0 with illumination, $n = 3$ cells, $n = 3$ animals).

The left cerebral cortex contralateral to the recorded PC was locally suppressed by systematic laser illumination during ION stimulation. As shown in Fig. 2, local illumination focused around the left SI (Fig. 2C–E) and MI (Fig. 2F–H) did not suppress the generation of CSs evoked by r-ION stimulation. Unexpectedly, illumination to the left MI showed a trend towards enhancing the generation of CSs (Fig. 2F–H). To confirm these results, we locally injected a GABA_A receptor agonist, muscimol, into the corresponding MI and SI area (see Methods). Muscimol was injected into both hemispheres in C57BL/6 mice to completely suppress the activity of these strongly interconnected areas (Fig. 3). Muscimol injections into the MI did not suppress but rather strongly enhanced CS generation by both r-ION and l-ION stimulation (Fig. 3A–C, G, I, J). In two of five PCs, two CSs were successively elicited within 100 ms after stimulation (Fig. 3A), which was never observed under control

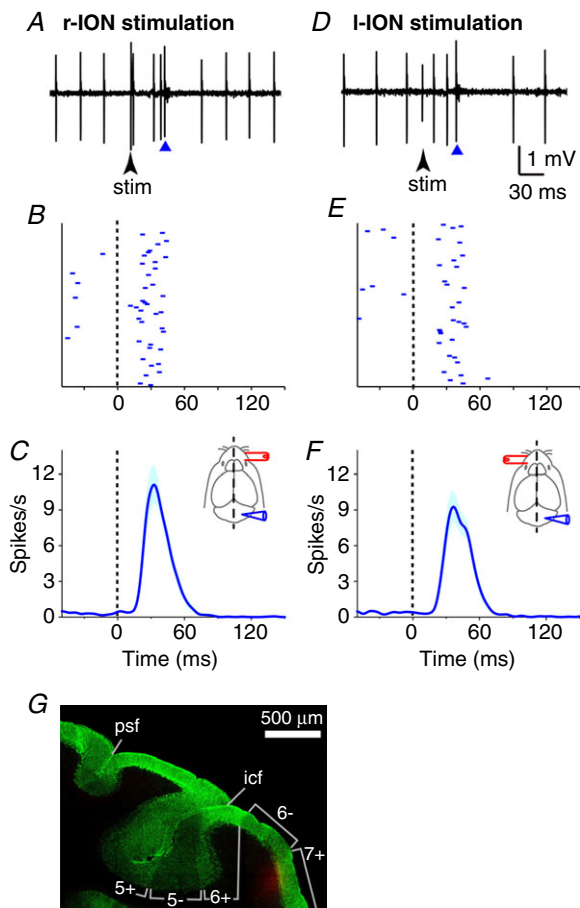


Figure 1. Complex spikes (CSs) generated by ipsilateral and contralateral infraorbital nerve (ION) stimulation

A and D, representative traces of CSs in response to a right ION (r-ION) (A) or a left ION (l-ION) (D) stimulation, which were recorded from the same Purkinje cell (PC) in the right Crus II. CSs are indicated by blue arrowheads. B and E, representative raster plots of CSs from 100 trials of r-ION (B) or l-ION (E) stimulation. Dotted lines represent ION stimulus onsets. C and F, peri-stimulus spike density functions (SDFs) of CSs in response to r-ION (C) or l-ION (F) stimulation ($n = 44$ cells, $n = 39$ animals). Blue lines and shaded areas indicate mean and SEM, respectively. Insets, schemas for stimulating (red) and recording (blue) sites. G, representative coronal section of the cerebellum immunostained with anti-aldolase C antibodies (green). The recording site is labelled with Alexa fluor 568 (red). In this mouse, the PC was recorded from the 7+ compartment. icf, intercrural fissure; psf, posterior superior fissure.

conditions. By contrast, bilateral muscimol injections into the SI were totally ineffective (Fig. 3D–F, H–J). Taken together, suppression of the MI and SI did not block signal transduction from the ION to the PCs via the IO, which suggests that the MI and the SI are not directly involved in the signalling pathway for the perioral sensory signal transduction from the ION to the IO. However, the MI suppression unexpectedly enhanced the generation of CSS

by ION stimulation, suggesting that the MI provides a suppressive influence on this anatomical pathway.

The PfPr is involved in the signal transduction pathway from the ION to the IO

The IO receives principally ipsilateral inputs from an area in the mesodiencephalic junction (Brown *et al.* 1977;

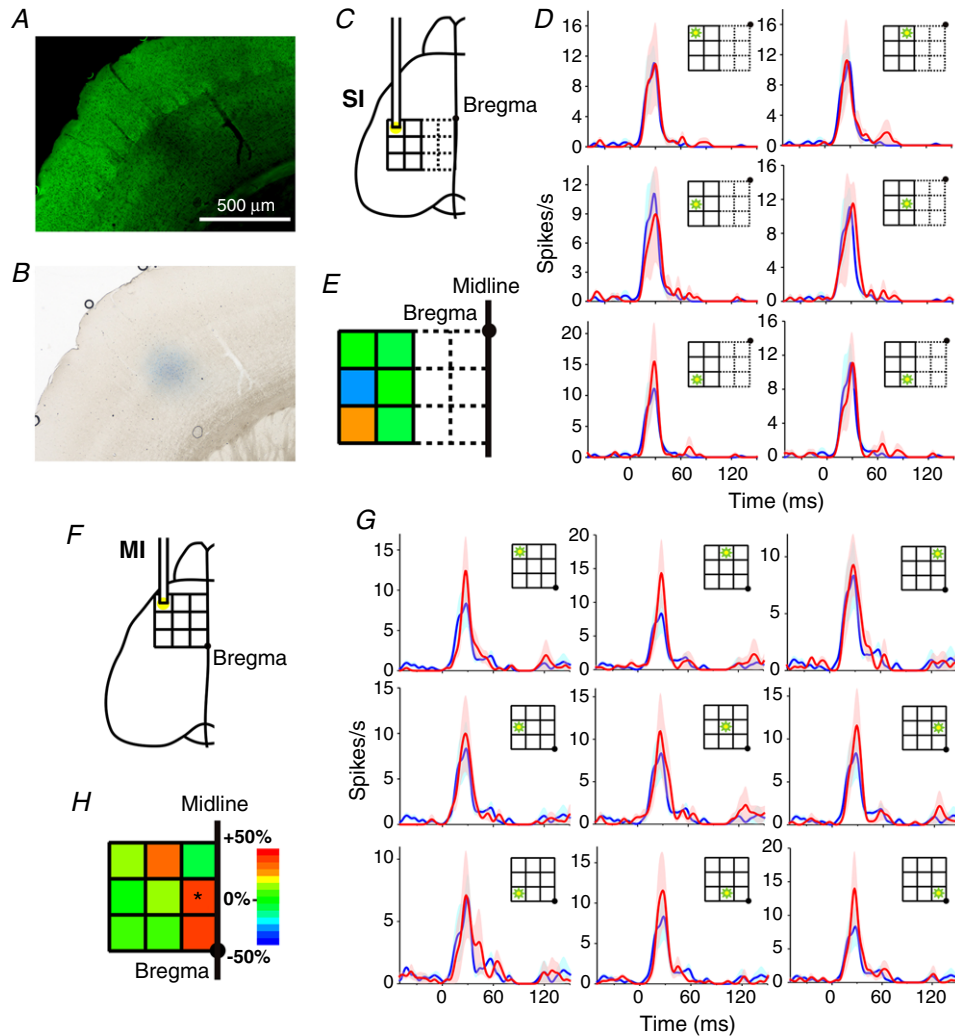


Figure 2. Effects of optogenetic inactivation of cortical pyramidal neurons on CS generation by r-ION stimulation

A and B, multi-unit recording site in the left primary somatosensory cortex (SI) identified by Chicago sky blue (B). A coronal slice of the SI in ArchT-EGFP expressing mice. ArchT-EGFP is strongly expressed in the entire cerebral cortex (A). In all experiments ($n = 3$ cells, $n = 3$ animals), recording electrodes were placed in layers V–VI. C and F, scheme for optical inactivation around the left SI (C) or motor (MI) cortex (F) contralateral to the recorded PC in ArchT-expressing mice. A 3×4 or 3×3 grid was placed on the SI or MI, respectively. For light illumination to the SI, six lateral grid columns were used. The pitch length of the grid was 1 mm. D and G, peri-stimulus SDFs of CSs in response to r-ION stimulation with (red) or without (blue) 575 nm light illumination to the left SI ($n = 3$ cells, $n = 3$ animals) (D) or MI ($n = 4$ cells, $n = 5$ animals) (G). Lines and shaded areas indicate mean and SEM, respectively. Insets indicate positions of light illumination. E and H, pseudocolour codes of the ratio of the difference of peak CS frequency between with and without light illumination relative to the peak CS frequency without the light illumination. The grid area marked with an asterisk indicates where the peak CS frequency with the light illumination was significantly higher than that without illumination ($*P = 0.032$, $n = 4$ pairs, $n = 5$ animals, paired *t*-test).

Cintas *et al.* 1980; Carlton *et al.* 1982; Swenson & Castro, 1983; Bentivoglio & Molinari, 1984; De Zeeuw *et al.* 1990; Paxinos, 2004), which is termed the PfPr (Carlton *et al.* 1982; Paxinos, 2004). If this area is involved in the tactile signalling pathway, the side contralateral to the recorded PCs should be activated because each PC receives a CF input from the contralateral IO. To test this hypothesis, we locally injected muscimol using a glass microelectrode to the l-PfPr contralateral to the recorded PC, and examined the influence on CS generation by r-ION stimulation (Fig. 4). We found that local muscimol injection into the l-PfPr around the ND and INC (0.5–1.2 mm rostral from the interaural line) strongly suppressed the generation of CSs by r-ION stimulation (Fig. 4A–D). In the thalamic region, neurons projecting to the IO are mainly distributed around the fr (Brown *et al.* 1977; Cintas *et al.* 1980; Carlton *et al.* 1982; Swenson & Castro, 1983; Bentivoglio & Molinari, 1984; De Zeeuw *et al.* 1990; Paxinos, 2004). Local muscimol injections into thalamic regions around the left fr (1.2–2.7 mm rostral from the interaural line) also strongly suppressed CSs generated by r-ION stimulation (Fig. 4C, E). This suppression was not observed in mice receiving vehicle injections (Fig. 4F). In addition, similar

muscimol injections to the right PfPr ipsilateral to the recorded PC were ineffective (Fig. 4C, G). The frequency of the spontaneous CSs was not significantly affected by muscimol injection (Fig. 4J). The distribution of effective injection sites roughly overlapped with the distribution of neurons directly projecting to the IO in rats (Brown *et al.* 1977; Cintas *et al.* 1980; Carlton *et al.* 1982; Swenson & Castro, 1983; Bentivoglio & Molinari, 1984; De Zeeuw *et al.* 1990; Paxinos, 2004). The IO is also known to receive inputs from the ipsilateral anterior pretectal area (Brown *et al.* 1977; Cintas *et al.* 1980; Swenson & Castro, 1983). However, muscimol injections focused on the left anterior pretectal area contralateral to the recorded PCs did not suppress the generation of CSs by r-ION stimulation (Fig. 4C, H). Taken together, these data suggest that the left mesodiencephalic junction relays sensory signals from the r-ION to the l-IO contralateral to the recorded PCs.

We also examined whether the sensory signal transduction was dependent on a vigilance state (Fig. 5). After surgery, mice were allowed to recover from anaesthesia, and then CS was recorded during the lightly anaesthetized state (see Methods). Under these conditions, the firing rate of spontaneous CSs was more

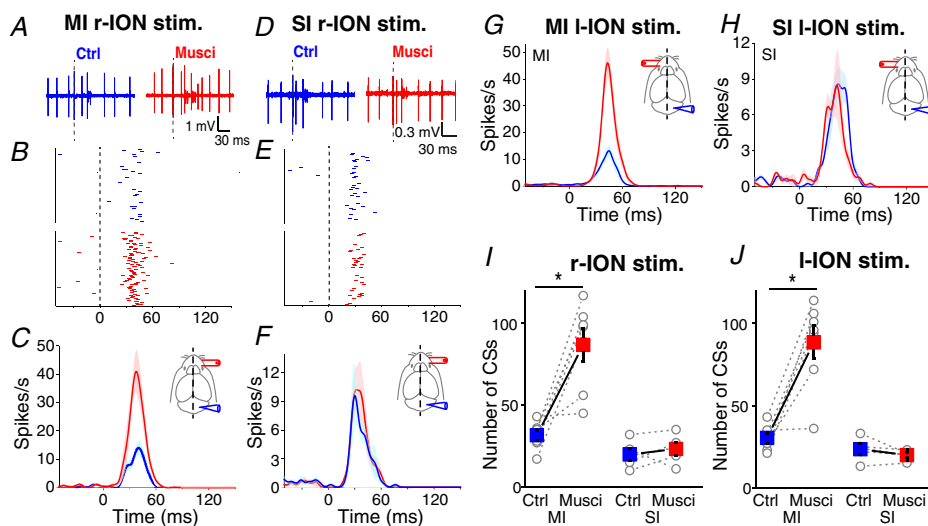


Figure 3. Effects of muscimol injections into the MI and SI on the generation of CSs by r-ION stimulation

A and D, representative traces of CSs in response to r-ION stimulation before (blue) and after (red) bilateral muscimol injections into the MI (A) or SI (D). In two of five PCs, some r-ION stimulations caused double CSs after muscimol injection into the MI. B and E, representative raster plots of CSs from 100 trials of r-ION stimulation before (blue) and after (red) bilateral muscimol injections into the MI (B) or SI (E). C and F, peri-stimulus SDFs of CSs in response to r-ION stimulation before (blue) and after (red) bilateral muscimol injections into the MI (C) or SI (F) ($n = 5$ cells, $n = 5$ animals). Lines and shaded areas indicate mean and SEM, respectively. Insets, schemas for stimulating (red) and recording (blue) sites. G and H, peri-stimulus SDFs of CSs in response to I-ION stimulation before (blue) and after (red) bilateral muscimol injections into the MI (G) ($n = 7$ cells, $n = 7$ animals) or SI (H) ($n = 5$ cells, $n = 5$ animals). Insets, schemas for stimulating (red) and recording (blue) sites. I and J, total number of CSs evoked by 100 r-ION (I) or I-ION (J) stimulations. Number of CSs during 0–100 ms after stimulus onset were counted. Averaged data for control (blue) and muscimol injected (red) are represented as mean \pm SEM. Muscimol injections into the MI (r-ION: $**P = 0.0032$, $n = 7$ pairs, $n = 7$ animals; I-ION: $**P = 0.0014$, $n = 7$ pairs, $n = 7$ animals; paired t -test), but not into the SI (r-ION: $P = 0.46$, $n = 5$ pairs, $n = 5$ animals; I-ION: $P = 0.2$, $n = 5$ pairs, $n = 5$ animals; paired t -test), significantly enhanced the incidence of CSs.

frequent than that in the deeply anaesthetized state (Figs 4J and 5D). The CSs evoked by r-ION stimulations were also significantly suppressed by muscimol injection to the l-PfPr, even in the lightly anaesthetized state (Fig. 5A–C).

Next, we examined the effect of muscimol injections into the l-PfPr on CS generation by l-ION stimulation. The effective regions for l-ION were more restricted compared with those for the r-ION (Fig. 6). Muscimol injections into the l-PfPr around the left INC (0.5–1.2 mm rostral from

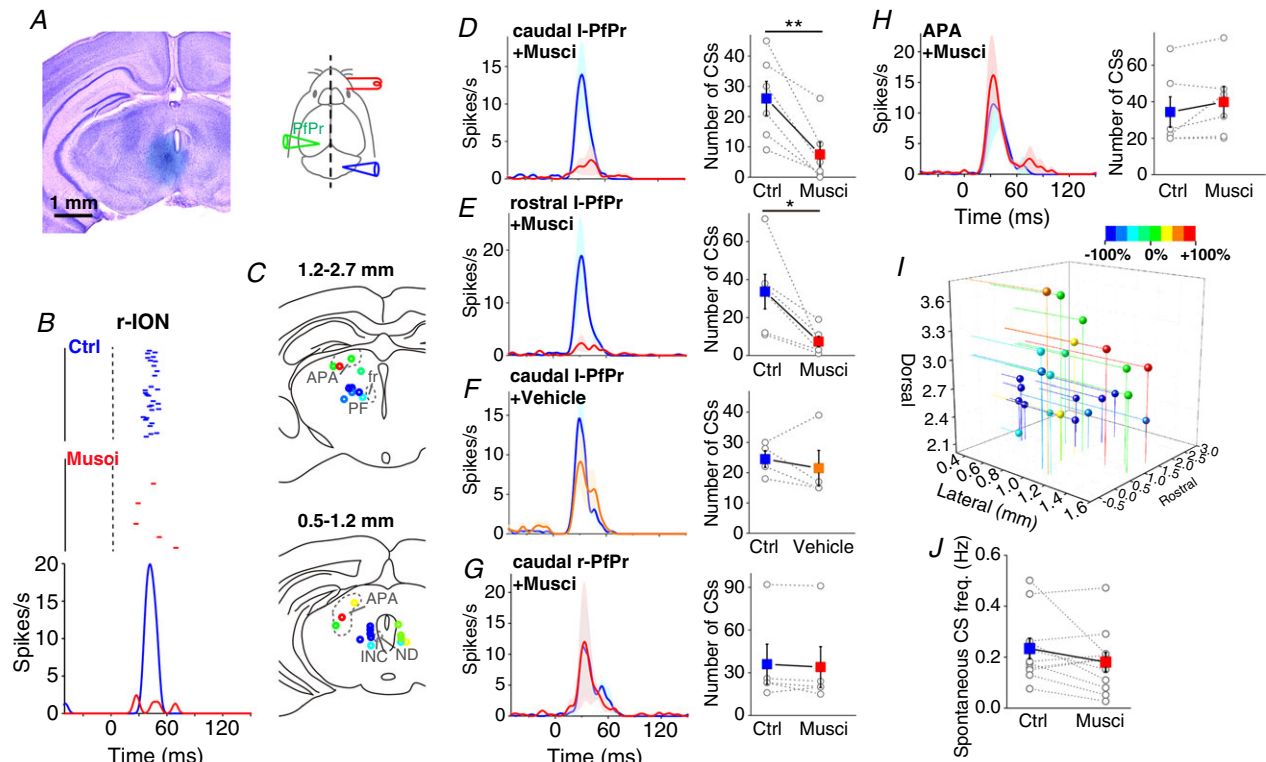


Figure 4. Muscimol injection into the area parafascicularis prerubralis (PfPr) significantly suppresses CS generation by r-ION stimulation

A, left, muscimol injection site identified by co-injected Chicago Sky Blue into the left PfPr (l-PfPr) surrounding the nucleus of Darkschewitsch (ND) and the interstitial nucleus of Cajal (INC). Right, schemas for stimulating (red), muscimol injection (green) and recording (blue) sites. B, representative raster plots (upper) and peri-stimulus SDFs (lower) of CSs from 100 trials of r-ION (left) stimulation before (blue) and after (red) muscimol injection into the l-PfPr shown in A. C, summary of centres of muscimol injection sites at 1.2–2.7 and 0.5–1.2 mm rostral to the interaural line. Pseudocolour codes of the ratio of the difference of the total CS number during 0–100 ms between before and after the muscimol injection relative to the total CS number before the muscimol injection. D, left, peri-stimulus SDFs of CSs in response to r-ION stimulation before (blue) and after (red) the muscimol injection into the caudal l-PfPr (0.5–1.2 mm rostral from interaural line, $n = 6$ cells, $n = 6$ animals). Right, total number of CSs during 100 ms after stimulus onsets evoked by 100 r-ION stimulations. The muscimol injection into the l-PfPr significantly suppressed CS generation by r-ION stimulation (** $P = 0.0064$, $n = 6$ pairs, $n = 6$ animals, paired t -test). E, similar to D, but data for muscimol injections into the rostral l-PfPr (1.2–2.7 mm rostral, $n = 6$ cells, $n = 6$ animals). Muscimol significantly suppressed CSs evoked by r-ION stimulation (* $P = 0.026$, $n = 6$ pairs, $n = 6$ animals, paired t -test). F, similar to D, but data for vehicle injections into the l-PfPr ($n = 4$ cells, $n = 4$ animals). The SDF after the vehicle injection is indicated in yellow. The CS generation was not significantly affected ($P = 0.54$, $n = 4$ pairs, $n = 4$ animals, paired t -test). G, similar to D, but data for muscimol injections into the right PfPr ($n = 5$ cells, $n = 5$ animals) ipsilateral to the recorded PC. The CS generation was not significantly affected ($P = 0.36$, $n = 5$ pairs, $n = 5$ animals, paired t -test). H, similar to D, but data for muscimol injections to the left anterior pretectal area ($n = 6$ cells, $n = 6$ animals) contralateral to the recorded PC. The CS generation was not significantly affected ($P = 0.19$, $n = 6$ pairs, $n = 6$ animals, paired t -test). I, summary of the effects of muscimol injections into the mesencephalic junction on CS generation. Rostral and dorsal values are distances from the interaural line. The lateral values are the distances from the midline. Colour coding is the same as that shown in C. J, averaged spontaneous CS frequency before (Ctrl) and after (Musci) muscimol injection ($n = 12$ cells, $n = 12$ animals). Only PCs whose CS generation by r-ION stimulation was reduced after muscimol injection were analysed. The frequency of the spontaneous CSs was not significantly affected by muscimol injection into the l-PfPr ($P = 0.056$, $n = 12$ pairs, $n = 12$ animals, paired t -test).

the interaural line) partially suppressed the generation of CSs by l-ION stimulation (Fig. 6B). In contrast, more rostral injections around the left fr (1.2–2.7 mm rostral from the interaural line) had little effect (Fig. 6C). These data suggest that convergence of signals from bilateral IONs at least partially occurs at or up to the relatively caudal part of the l-PfPr.

Electrophysiological and morphological analyses of input–output pathways for the PfPr

To confirm the existence of a functional projection from the l-PfPr to the l-IO, the l-PfPr was electrically stimulated by a monopolar glass microelectrode. As expected, electrical stimulation of the l-PfPr evoked CSs (Fig. 7A, C, E), indicating the existence of functional connections from the l-PfPr to the l-IO (Jeneskog, 1987; Ruigrok *et al.* 1990). The shortest latency of the CS firing for l-PfPr stimulation was significantly faster than that for r-ION stimulation recorded in the same PCs (paired *t*-test) (Fig. 7B, D, F). These data support the notion that the PfPr-IO pathway is directly involved in the signal

transduction pathway from the ION to the IO. The SDFs of the CSs had two major peaks at latencies of 15 and 40 ms (Fig. 7C). The peak of the first component was also clearly earlier than that of CSs elicited by ION stimulation (30 ms) recorded from the same PCs. It is unclear whether the second peak was evoked by direct projections to the IO. It remains a possibility that the artificial electrical stimulation may activate longer unidentified signalling pathways.

To confirm the output anatomical pathways from the l-PfPr to the l-IO, an anterograde tracer, BDA, was injected into the l-PfPr where muscimol injections suppressed CS generation by both r-ION and l-ION stimulations (Fig. 8). Previous reports have demonstrated that some subnuclei in the PfPr provide strong projections to the rostral area of the medial accessory olive (MAO), dorsal and ventral lamella of the principal olive (PO), and dorso-medial cell column in rats (Cintas *et al.* 1980; Carlton *et al.* 1982; Swenson & Castro, 1983; De Zeeuw *et al.* 1990; Paxinos, 2004). Our results confirm these previous findings. Strongly labelled axons distributed in the relatively rostral area of the ipsilateral IO. They distributed in the MAO, the ventral lamella of the PO and a part of the dorsal lamella of the PO (Fig. 8B–D). Because D1–D2 zones receive CFs from the ventral and dorsal lamella of the PO and the dorsomedial group subnucleus (Huerta *et al.* 1983; Buisseret-Delmas & Angaut, 1993; Sugihara *et al.* 2007), these data confirm that neurons in the PfPr send axons to the ipsilateral IO areas projecting to the Crus II.

Next, we examined the inputs to the PfPr by local injections of a retrograde tracer, FG (Fig. 9). Retrogradely labelled FG-positive neurons were observed in the contralateral side of the SpVo (Fig. 9B, C), but not in the SpVi (Fig. 9D, E) or the SpVc (Fig. 8F, G). Taken together, these results indicate that the PfPr is involved in the anatomical pathway from the trigeminal nuclei to PCs via the IO.

CSs evoked by mechanical stimulation of the perioral whisker region are also suppressed by muscimol injections into the PfPr

Finally, we tested whether muscimol injection into the l-PfPr suppressed CS generation by a more natural type of stimulation (Fig. 10). CSs were elicited by air-puffs to the perioral region instead of electrical stimulation to the r-ION and l-ION. The latency of CSs evoked by right and left air-puff stimulation were 50.3 ± 6.6 and 57.0 ± 10.9 ms, respectively ($n = 6$ cells, $n = 6$ animals; Fig. 10B–E). CSs evoked by right and left air-puff stimulation were effectively suppressed by local injections of muscimol into the caudal part of the l-PfPr (Fig. 10), which indicates that the PfPr is involved in tactile signal transduction from the perioral area to PCs via the contralateral IO.

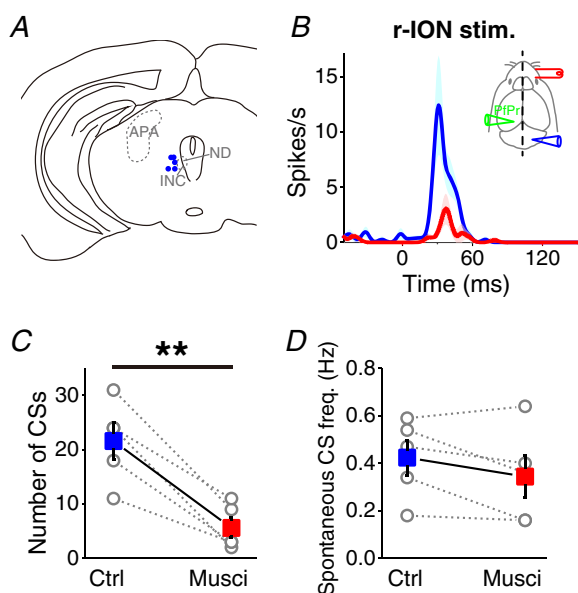


Figure 5. Muscimol injection to the PfPr in lightly anaesthetized mice

A, summary of muscimol injection sites. B, averaged peri-stimulus SDFs in response to r-ION stimulation before (blue) and after (red) muscimol injection into the caudal l-PfPr ($n = 5$ cells, $n = 5$ animals) in lightly anaesthetized mice. Lines and shaded areas indicate mean and SEM, respectively. Insets, schemas for stimulating and recording sites. C, Total number of CSs during 100 ms after stimulus onsets evoked by 100 r-ION stimulations before (Ctrl) and after (Musci) muscimol injection (** $P = 0.0041$, $n = 5$ pairs, $n = 5$ animals, paired *t*-test). D, averaged spontaneous CS frequency before (Ctrl) and after (Musci) muscimol injection. The frequency of the spontaneous CSs was not significantly affected by muscimol injection into the l-PfPr ($P = 0.14$, $n = 5$ pairs, $n = 5$ animals, paired *t*-test).

Discussion

The PfPr relays perioral sensory signals to the IO

Effective muscimol injection sites for r-ION stimulation closely overlapped the distribution of IO-projecting neurons in the mesodiencephalic junction (Fig. 4C, D, E) (Brown *et al.* 1977; Cintas *et al.* 1980; Carlton *et al.* 1982; Swenson & Castro, 1983; Bentivoglio & Molinari, 1984; De Zeeuw *et al.* 1990; Paxinos, 2004). Previous studies have demonstrated that the mesencephalic reticular formation, the ND and the PF in the PfPr receive direct anatomical inputs from the SpVs (Veazey & Severin, 1982; Onodera & Hicks, 1995; Krout *et al.* 2002). We also confirmed the existence of a direct projection from the contralateral SpVo (Fig. 9B, C). The SpVo contains neurons that respond to light mechanical stimulation of the perioral and intra-oral area in rats (Dallel *et al.* 1990). Mechanoreceptive neurons responding to the perioral area are mainly distributed in the ventrolateral part of the SpVo (Dallel

et al. 1990). Neurons in this region were retrogradely labelled by FG injection into the contralateral PfPr (Fig. 9B, C). These data suggest the existence of a direct signalling pathway from the contralateral SpVo to the PfPr.

In addition, our electrophysiological (Fig. 7) and morphological (Fig. 8) analyses confirmed the existence of a functional projection from the PfPr to the ipsilateral IO. Many previous reports have also demonstrated that neurons in the PfPr have principally ipsilateral strong projections to the MAO and the PO in the rostral area of the IO (Cintas *et al.* 1980; Carlton *et al.* 1982; Swenson & Castro, 1983; De Zeeuw *et al.* 1990; Paxinos, 2004) (Fig. 8). At least some of these synaptic inputs from around the ND to the IO are excitatory (Cintas *et al.* 1980; De Zeeuw *et al.* 1989, 1990). In the present study, the IO areas receiving inputs from the PfPr cover the MAO and the ventral and a part of the dorsal lamellas of the PO in the relatively rostral part of the IO, which project to the contralateral

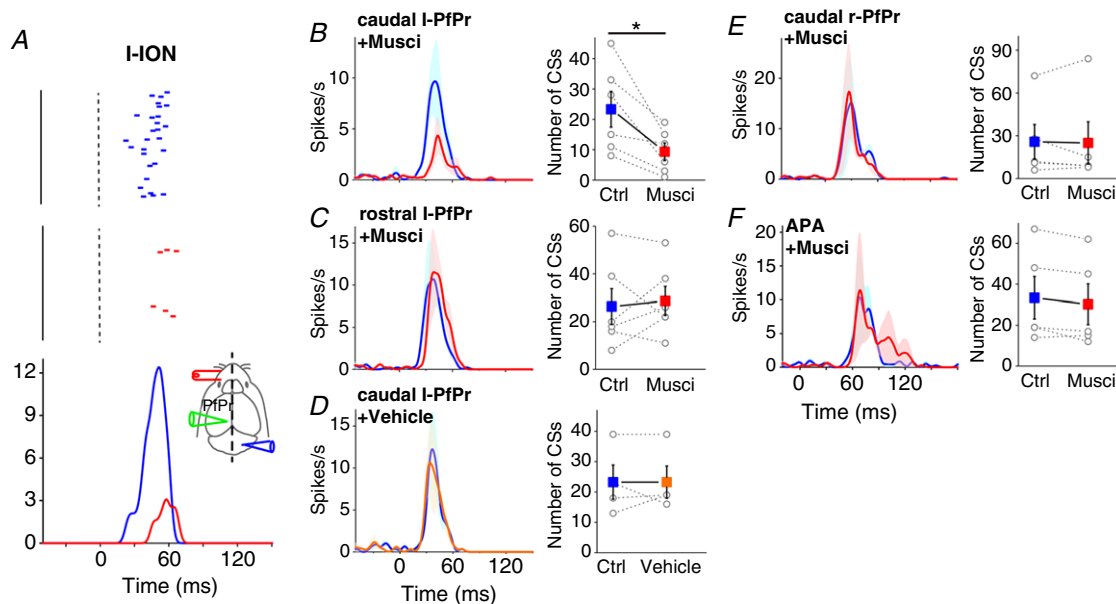


Figure 6. Effects of muscimol injection to the PfPr on the CS generation by I-ION stimulation

A, representative raster plots (upper) and peri-stimulus SDFs (lower) of CSs from 100 trials of I-ION stimulation before (blue) and after (red) muscimol injection into the I-PfPr shown in Fig. 4A. Insets, schemas for stimulating (red), muscimol injection (green) and recording (blue) sites. B, left, peri-stimulus SDFs of CSs in response to I-ION stimulation before (blue) and after (red) the muscimol injection into the caudal I-PfPr (0.5–1.2 mm rostral from interaural line, $n = 6$ cells, $n = 6$ animals). Right, total number of CSs during 100 ms after stimulus onsets evoked by 100 I-ION stimulations. The muscimol injection into the caudal I-PfPr significantly suppressed CS generation by I-ION stimulation ($*P = 0.024$, $n = 6$ pairs, $n = 6$ animals, paired t -test). C, similar to B, but data for muscimol injections into the rostral I-PfPr (1.2–2.7 mm rostral, $n = 6$ cells, $n = 6$ animals). Muscimol did not suppress CSs evoked by I-ION stimulation ($P = 0.69$, $n = 6$ pairs, $n = 6$ animals, paired t -test). D, similar to B, but data for vehicle injections into the I-PfPr ($n = 4$ cells, $n = 4$ animals). The SDF after the vehicle injection is indicated in yellow. The CS generation was not significantly affected ($P = 1.00$, $n = 4$ pairs, $n = 4$ animals, paired t -test). E, similar to B, but data for muscimol injections into the right PfPr ($n = 5$ cells, $n = 5$ animals) ipsilateral to the recorded PC. The CS generation was not significantly affected ($P = 0.85$, $n = 5$ pairs, $n = 5$ animals, paired t -test). F, similar to B, but data for muscimol injections to the left anterior pretectal area ($n = 5$ cells, $n = 5$ animals) contralateral to the recorded PC. The CS generation was not significantly affected ($P = 0.078$, $n = 5$ pairs, $n = 5$ animals, paired t -test).

Crus II (Huerta *et al.* 1983; Buisseret-Delmas & Angaut, 1993; Sugihara *et al.* 2007).

According to previous reports in rats, the latency of spikes evoked by mechanical stimulations to the face is 3.7 ms in SpVo neurons (Dallel *et al.* 1990). McClung & Dafny (1980) reported that SpV stimulations evoked action potentials in the PF, with the shortest latency of approximately 10 ms estimated from a representative trace and the histogram. In the present study, the shortest latency of CSs calculated from the SDF between the PfPr and the PC was approximately 10 ms (Fig. 7). The calculated total latency from the perioral area to the PC is comparable with that of the CS latency after ION stimulations (21 ms) in the present study. We think that the delay of CSs in response to ION stimulation is reasonably explained by signal transduction via the PfPr. Taken together, these findings suggest that the perioral tactile signal ipsilateral to the recorded PC can be transmitted through the ipsilateral SpVo, the l-PfPr and the l-IO.

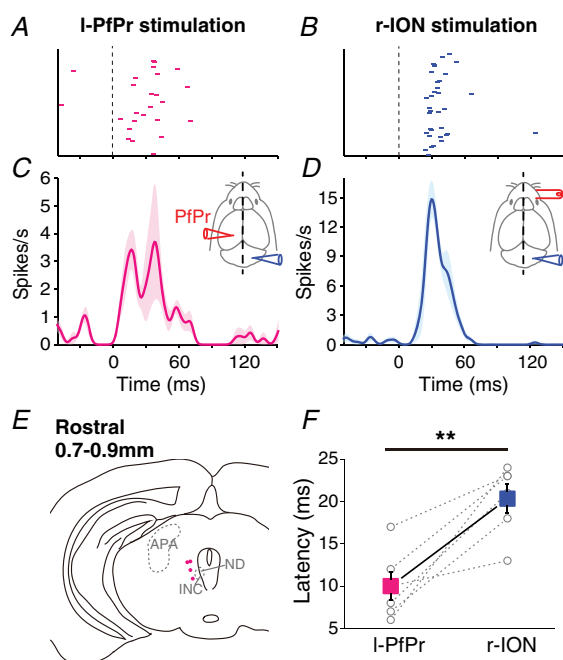


Figure 7. Electrical stimulation of the PfPr evokes CSs

A and B, representative raster plots of CSs from 100 trials of l-PfPr (A) or r-ION (B) stimulation recorded from the same PC. C and D, averaged peri-stimulus SDFs in response to l-PfPr (C) or r-ION (D) stimulation ($n = 6$ cells, $n = 4$ animals). Lines and shaded areas indicate mean and SEM, respectively. Insets, schemas for stimulating (red) and recording (blue) sites. E, summary of contralateral PfPr stimulation sites (pink dots). F, latencies of CSs in response to l-PfPr or r-ION stimulation. The start of the CS firing was assessed by the latency when the SDF exceeded the mean ± 2 SD of baseline frequency for 50 s. Latency for PfPr stimulation was significantly shorter than that for r-ION stimulation (** $P = 0.0049$, $n = 6$ pairs, $n = 4$ animals, paired t -test).

Inhibition of the l-PfPr also partially suppressed the CS generation evoked by l-ION stimulation (Fig. 6B). However, the effective injection sites were restricted to around the relatively caudal part of the l-PfPr (Fig. 6B, C). Because identified projections from the PfPr to the IO are principally ipsilateral, and muscimol injections to the ipsilateral PfPr did not affect CS generation, the signalling pathway from the l-ION passes, at least partly, through the relatively caudal part of the l-PfPr. In the present study, because FG-labelled neurons were mainly distributed in the SpVo contralateral to the injected PfPr, signals from l-ION may not be directly transmitted from the left SpVs to the l-PfPr but relayed at one or more additional brain regions. This may cause the relatively longer latency of the l-ION compared with that of the r-ION. However, according to previous reports (Veazey & Severin, 1982; Onodera & Hicks, 1995), it remains a possibility that PfPr receives direct ipsilateral projections from SpVs.

MI suppresses the signalling pathway from the ION to the IO

In the present study, the optical inhibition or muscimol injection into the MI or SI did not block the incidence of CSs by ION stimulation in the anaesthetized mice (Fig. 3), suggesting that the MI and SI are not directly involved in the sensory signalling pathway from the ION to the IO. However, anaesthesia might suppress signal transduction through more complex and longer pathways (Sasaki *et al.* 1975). Therefore, we applied muscimol to the PfPr in lightly anaesthetized mice and found that CS generation was also significantly suppressed in this situation (Fig. 5). These data suggest that most sensory signals from the ION to the IO are transmitted through the PfPr even in the lightly anaesthetized state.

However, the data do not completely rule out the existence of more complex and longer signal transduction pathways between the ION and the PfPr. In the lightly anaesthetized state, the signalling pathway through the cerebral cortex might be disinhibited and relay sensory signals to the PfPr. Furthermore, sensory signals may be relayed at areas not experimentally manipulated in the present study. The optically inactivated area largely covered the vibrissal MI area but might not reach rostral and caudal edges of the MI (Fig. 2). The small rostral area of the SI might also not be optically inactivated. In cats, neurons in the motor cortex form synapses on the ND neurons projecting to the MAO (Nakamura *et al.* 1983). In addition, there are other cortical areas for which stimulation can evoke CSs, such as the parietal cortex (Sasaki *et al.* 1975; Oka *et al.* 1979). Involvement of the cerebral cortex in the sensory signalling pathway should be carefully addressed in future studies.

Muscimol injection into the MI rather strongly enhanced the generation of CSs, which suggests that the MI suppresses the signalling pathway from the ION to PCs via the IO. Similar cortical inhibition was also observed in cats. Leicht *et al.* (1973) demonstrated that pericruciate cortical stimulation at subthreshold levels for CS generation suppressed the generation of CSs evoked

by hind limb tactile stimulation. Although the signalling pathway from the hindlimb to the IO is different from that in the present study, sensory transduction via the IO may be similarly regulated by the cerebral cortex. The signalling pathway for the MI-dependent suppression is currently unclear. Previous studies suggest that some nuclei in the PfPr are innervated by cerebral cortical neurons (Veazey

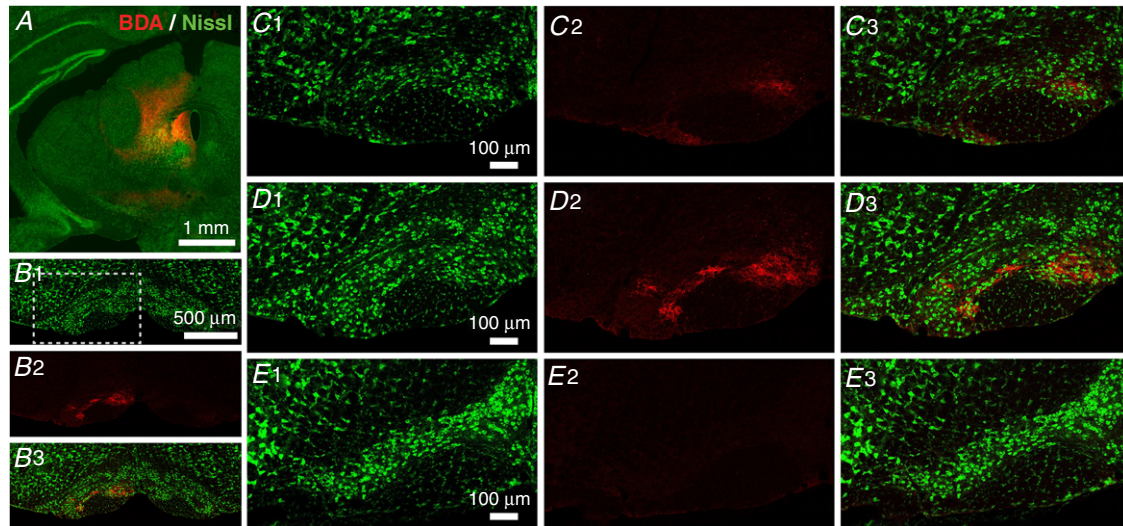


Figure 8. Anterograde tracer injections into the PfPr

Biotinylated dextran amine (BDA) anterograde tracer labelling of outputs from the contralateral (left) PfPr. *A*, double-labelling of the representative injection site for BDA (red) and Nissl bodies (green). *B*, double-labelling for Nissl bodies (*B1*, green) and BDA (*B2*, red) in the IO. Images are merged in *B3*. BDA-labelled axons are observed in the IO ipsilateral to the injection sites. *C–E*, enlarged images at the rostral (*C*), middle (*D*) and caudal (*E*) parts of the IO. The image in *D* is the enlarged image of the boxed area in *B*. Similar staining was observed in four mice.

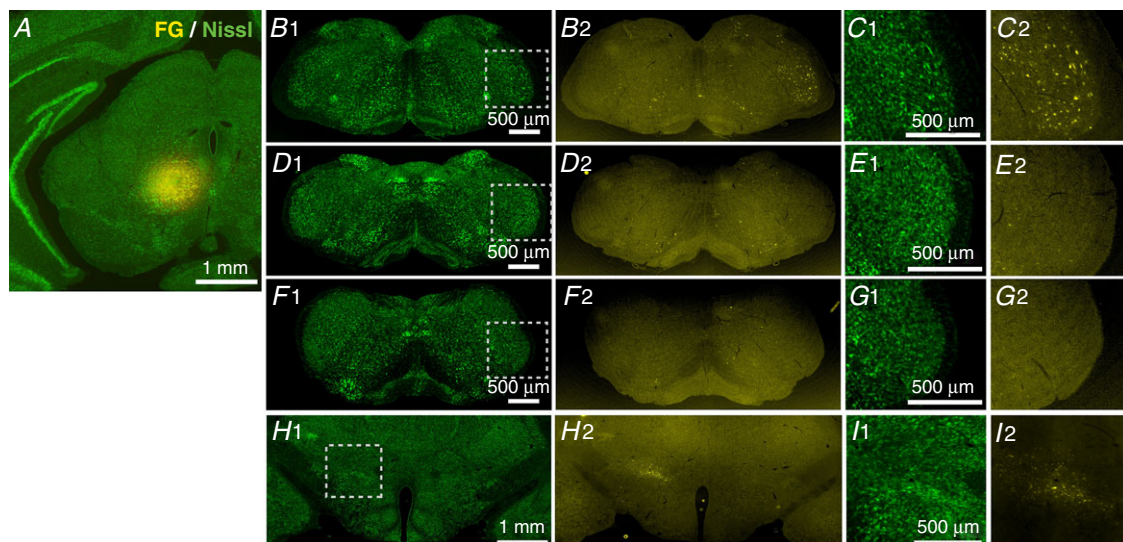


Figure 9. Retrograde tracer injections into the PfPr

Fluoro-Gold (FG) retrograde tracer labelling of inputs into the I-PfPr. *A*, double-labelling of the representative injection site for FG (yellow) and Nissl bodies (green). *B–I*, double-labelling for Nissl bodies (green) and FG-positive cells (yellow) in the SpVo (*B*), SpVi (*D*), SpVc (*F*) and zona incerta (*H*). Enlarged images of the boxed areas in *B1*, *D1*, *F1* and *H1* are shown in *C*, *E*, *G* and *I*, respectively. FG-labelled neurons are observed in the SpVo (*B*, *C*) and zona incerta (*H*, *I*), but not in the SpVi (*D*, *E*) or SpVc (*F*, *G*). Similar staining was observed in four mice.

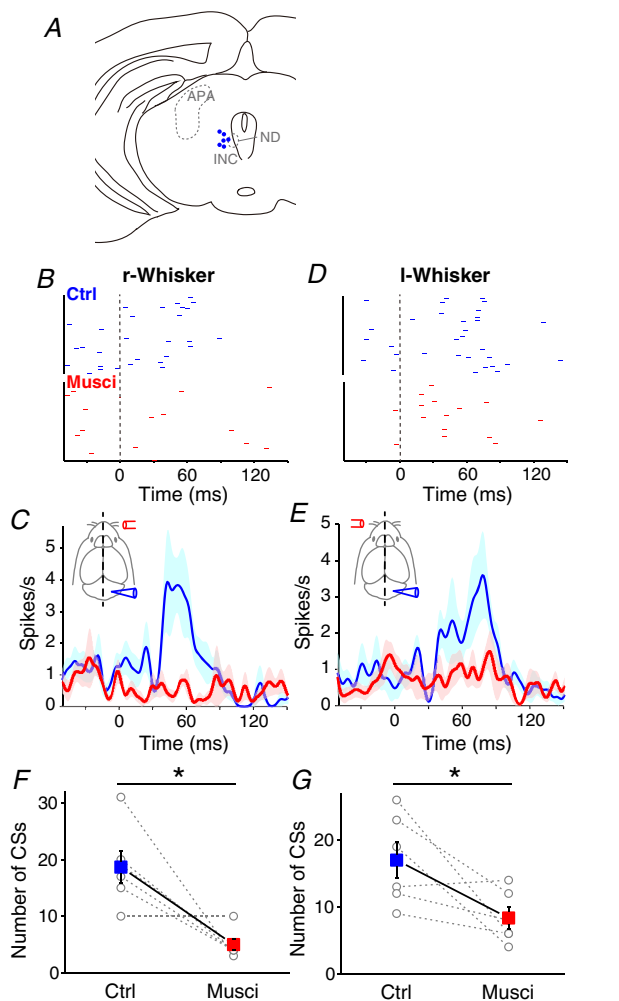


Figure 10. Effects of muscimol injections into the I-PfPr on CSs evoked by air-puffs to the perioral region

A, summary of muscimol injection sites (blue dots) in the I-PfPr. B, representative raster plots of CSs in 100 trials of right perioral stimulation by air-puffs (5 ms, 0.34 MPa). C, peri-stimulus SDFs of CSs evoked by right perioral stimulation before (blue) and after (red) the muscimol injection ($n = 6$ cells, $n = 6$ animals). Lines and shaded areas indicate mean and SEM, respectively. Insets, schemas for stimulating (red), muscimol injection (green) and recording (blue) sites. D, representative raster plots of CSs evoked from 100 trials of left perioral stimulation, which were recorded from the same neuron shown in B. E, peri-stimulus SDFs of CSs evoked by left perioral stimulation before (blue) and after (red) the muscimol injection ($n = 6$ cells, $n = 6$ animals). F and G, total number of CSs evoked by 100 right (F) or left (G) perioral stimulation. CSs during 0–100 ms after stimulus onset were counted. Averaged data for control (blue) and muscimol injected (red) are represented as mean \pm SEM. Muscimol injection into the I-PfPr significantly suppressed CSs evoked by right (ipsilateral) and left (contralateral) perioral stimulation (right: $*P = 0.014$; left: $*P = 0.046$; $n = 6$ pairs, $n = 6$ animals, paired t -test).

& Severin, 1982; Nakamura *et al.* 1983; Saint-Cyr, 1987; Stuesse & Newman, 1990; Onodera & Hicks, 1995), but it is not clear whether this direct innervation has an inhibitory influence on this signalling pathway. Interestingly, neurons likely in the zona incerta ipsilateral from the injection site were labelled by FG injections into the PfPr (Fig. 9H, I). Because neurons in the zona incerta are GABAergic and receive projections from the motor and somatosensory cortex (Urbain & Deschenes, 2007), the zona incerta may be a candidate relay for the inhibitory pathway from the MI.

Anatomical pathways for conducting the perioral tactile signal to the IO

It is unlikely that the pathway via the mesodiencephalic junction is the sole pathway for conduction of perioral sensory signalling to the IO. In the present study, r-ION and l-ION stimulation were both effective in evoking CSs, but the preference of ipsilateral and contralateral perioral stimulation differs among previous reports (Miles & Wiesendanger, 1975a; Cook & Wiesendanger, 1976; Armstrong & Drew, 1980; Mulle *et al.* 1987; Akaike, 1988; Thomson *et al.* 1989; Brown & Bower, 2001; Bosman *et al.* 2010), suggesting that projection patterns from the left and right perioral areas are variable among PCs.

Importantly, the IO receives direct innervation principally from contralateral SpVs. Previous morphological analyses suggest that axons from the SpVs innervate the dorsomedial part of the rostral dorsal accessory olive, the dorsomedial part of the dorsal lamella of the PO and the dorsomedial group of the ventral lamella of the PO (Huerta *et al.* 1983; Swenson & Castro, 1983; De Zeeuw *et al.* 1996; Molinari *et al.* 1996; Yatim *et al.* 1996), which send projections to the C3, D0 and D1 zones, but not to the C2 and D2 zones, in the Crus II (Sugihara & Quy, 2007; Sugihara *et al.* 2007; Bosman *et al.* 2010). Therefore, the contribution of the direct SpVs–IO pathway would change depending on the recording site of PCs in Crus II. In the present study, PCs were mainly sampled from zones receiving CFs from IO regions with (D1) or without (D2) SpV projections (see Methods). Although we assumed that the signal transduction via the direct SpVs to the IO pathway would show a shorter latency because of its shorter conduction length, the latencies of the CSs were identical between these groups (D1: 36.9 ± 5.2 ms, $n = 4$ cells; D2: 41.3 ± 8.1 ms, $n = 5$ cells) in the present study. These data suggest that the contribution of the direct SpV–olivary pathway may not be simply determined by anatomical innervation territories. It is unclear how the direct SpV–olivary pathway is activated, but it may depend on the sensory modality. SpVs, especially SpVc, are known to be crucial for nociception, and thus the

direct pathway may be involved in some sort of the nociceptive signal transduction to the cerebellum via CFs (Ekerot *et al.* 1987).

The functional role of the PfPr in sensory signal processing is currently unclear. However, the projection from the PfPr to the IO is well conserved in the cat, opossum, mouse, rat and monkey (Henkel *et al.* 1975; Linauts & Martin, 1978; Cintas *et al.* 1980; Saint-Cyr & Courville, 1981; Kokkoroyannis *et al.* 1996), indicating the functional importance of this network. In addition, the PfPr is an area that receives inputs from both the cerebral cortex (Veazey & Severin, 1982; Nakamura *et al.* 1983; Saint-Cyr, 1987; Stuesse & Newman, 1990; Onodera & Hicks, 1995) and deep cerebellar nuclei (Gonzalo-Ruiz *et al.* 1990; Ruigrok & Voogd, 1995; Ruigrok & Teune, 2014), and thus the sensory signals are assumed to be subject to multiple modulation by higher brain regions. These lines of evidence suggest the importance of this network in cerebellar functions.

References

- Ackerley R, Pardoe J & Apps R (2006). A novel site of synaptic relay for climbing fibre pathways relaying signals from the motor cortex to the cerebellar cortical C1 zone. *J Physiol* **576**, 503–518.
- Akaike T (1988). Electrophysiological analysis of the trigemino-tecto-olivo-cerebellar (crus II) projection in the rat. *Brain Res* **442**, 373–378.
- Armstrong DM & Drew T (1980). Responses in the posterior lobe of the rat cerebellum to electrical stimulation of cutaneous afferents to the snout. *J Physiol* **309**, 357–374.
- Bentivoglio M & Molinari M (1984). The interrelations between cell groups in the caudal diencephalon of the rat projecting to the striatum and to the medulla oblongata. *Exp Brain Res* **54**, 57–65.
- Bosman LW, Houweling AR, Owens CB, Tanke N, Shevchouk OT, Rahmati N, Teunissen WH, Ju C, Gong W, Koekkoek SK & De Zeeuw CI (2011). Anatomical pathways involved in generating and sensing rhythmic whisker movements. *Front Integr Neurosci* **5**, 53.
- Bosman LW, Koekkoek SK, Shapiro J, Rijken BF, Zandstra F, van der Ende B, Owens CB, Potters JW, de Gruilj JR, Ruigrok TJ & De Zeeuw CI (2010). Encoding of whisker input by cerebellar Purkinje cells. *J Physiol* **588**, 3757–3783.
- Brown IE & Bower JM (2001). Congruence of mossy fiber and climbing fiber tactile projections in the lateral hemispheres of the rat cerebellum. *J Comp Neurol* **429**, 59–70.
- Brown JT, Chan-Palay V & Palay SL (1977). A study of afferent input to the inferior olivary complex in the rat by retrograde axonal transport of horseradish peroxidase. *J Comp Neurol* **176**, 1–22.
- Buisseret-Delmas C & Angaut P (1993). The cerebellar olivo-corticonuclear connections in the rat. *Progr Neurobiol* **40**, 63–87.
- Carlton SM, Leichnetz GR & Mayer JD (1982). Projections from the nucleus parafascicularis prerubralis to medullary raphe nuclei and inferior olive in the rat: a horseradish peroxidase and autoradiography study. *Neurosci Lett* **30**, 191–197.
- Cintas HM, Rutherford JG & Gwyn DG (1980). Some midbrain and diencephalic projections to the inferior olive in the rat. In *The Inferior Olivary Nucleus, Anatomy and Physiology*, ed. Courville J, de Montigny C & Lamarre Y, pp. 73–96. Raven Press, New York.
- Cook JR & Wiesendanger M (1976). Input from trigeminal cutaneous afferents to neurones of the inferior olive in rats. *Exp Brain Res* **26**, 193–202.
- Dalle R, Raboisson P, Woda A & Sessle BJ (1990). Properties of nociceptive and non-nociceptive neurons in trigeminal subnucleus oralis of the rat. *Brain Res* **521**, 95–106.
- De Zeeuw CI, Holstege JC, Ruigrok TJ & Voogd J (1989). Ultrastructural study of the GABAergic, cerebellar, and mesodiencephalic innervation of the cat medial accessory olive: anterograde tracing combined with immunocytochemistry. *J Comp Neurol* **284**, 12–35.
- De Zeeuw CI, Holstege JC, Ruigrok TJ & Voogd J (1990). Mesodiencephalic and cerebellar terminals terminate upon the same dendritic spines in the glomeruli of the cat and rat inferior olive: an ultrastructural study using a combination of [³H]leucine and wheat germ agglutinin coupled horseradish peroxidase anterograde tracing. *Neuroscience* **34**, 645–655.
- De Zeeuw CI, Lang EJ, Sugihara I, Ruigrok TJ, Eisenman LM, Mugnaini E & Llinas R (1996). Morphological correlates of bilateral synchrony in the rat cerebellar cortex. *J Neurosci* **16**, 3412–3426.
- Diamond ME & Arabzadeh E (2013). Whisker sensory system - from receptor to decision. *Progr Neurobiol* **103**, 28–40.
- Ekerot CF, Oscarsson O & Schouenborg J (1987). Stimulation of cat cutaneous nociceptive C fibres causing tonic and synchronous activity in climbing fibres. *J Physiol* **386**, 539–546.
- Feldmeyer D, Brecht M, Helmchen F, Petersen CC, Poulet JF, Staiger JF, Luhmann HJ & Schwarz C (2013). Barrel cortex function. *Progr Neurobiol* **103**, 3–27.
- Gonzalo-Ruiz A, Leichnetz GR & Hardy SG (1990). Projections of the medial cerebellar nucleus to oculomotor-related midbrain areas in the rat: an anterograde and retrograde HRP study. *J Comp Neurol* **296**, 427–436.
- Henkel CK, Linauts M & Martin GF (1975). The origin of the annulo-olivary tract with notes on other mesencephalo-olivary pathways. A study by the horseradish peroxidase method. *Brain Res* **100**, 145–150.
- Huerta MF, Frankfurter A & Harting JK (1983). Studies of the principal sensory and spinal trigeminal nuclei of the rat: projections to the superior colliculus, inferior olive, and cerebellum. *J Comp Neurol* **220**, 147–167.
- Iwasato T, Datwani A, Wolf AM, Nishiyama H, Taguchi Y, Tonegawa S, Knopfel T, Erzurumlu RS & Itoharu S (2000). Cortex-restricted disruption of NMDAR1 impairs neuronal patterns in the barrel cortex. *Nature* **406**, 726–731.
- Jeneskog T (1987). Termination in posterior and anterior cerebellum of a climbing fibre pathway activated from the nucleus of Darkschewitsch in the cat. *Brain Res* **412**, 185–189.

- Kassai H, Terashima T, Fukaya M, Nakao K, Sakahara M, Watanabe M & Aiba A (2008). Rac1 in cortical projection neurons is selectively required for midline crossing of commissural axonal formation. *Eur J Neurosci* **28**, 257–267.
- Kleinfeld D & Deschenes M (2011). Neuronal basis for object location in the vibrissa scanning sensorimotor system. *Neuron* **72**, 455–468.
- Kokkoroyannis T, Scudder CA, Balaban CD, Highstein SM & Moschovakis AK (1996). Anatomy and physiology of the primate interstitial nucleus of Cajal I. efferent projections. *J Neurophysiol* **75**, 725–739.
- Krout KE, Belzer RE & Loewy AD (2002). Brainstem projections to midline and intralaminar thalamic nuclei of the rat. *J Comp Neurol* **448**, 53–101.
- Lang EJ (2001). Organization of olivocerebellar activity in the absence of excitatory glutamatergic input. *J Neurosci* **21**, 1663–1675.
- Leicht R, Rowe MJ & Schmidt RF (1973). Cortical and peripheral modification of cerebellar climbing fibre activity arising from cutaneous mechanoreceptors. *J Physiol* **228**, 619–635.
- Linauts M & Martin GF (1978). An autoradiographic study of midbrain-diencephalic projections to the inferior olivary nucleus in the opossum (*Didelphis virginiana*). *J Comp Neurol* **179**, 325–353.
- McClung RE & Dafny N (1980). The parafascicular nucleus of thalamus exhibits convergence input from the dorsal raphe and the spinal tract of the trigeminal nerve. *Brain Res* **197**, 525–531.
- Miles TS & Wiesendanger M (1975a). Climbing fibre inputs to cerebellar Purkinje cells from trigeminal cutaneous afferents and the SI face area of the cerebral cortex in the cat. *J Physiol* **245**, 425–445.
- Miles TS & Wiesendanger M (1975b). Organization of climbing fibre projections to the cerebellar cortex from trigeminal cutaneous afferents and from the SI face area of the cerebral cortex in the cat. *J Physiol* **245**, 409–424.
- Molinari HH, Schultze KE & Strominger NL (1996). Gracile, cuneate, and spinal trigeminal projections to inferior olive in rat and monkey. *J Comp Neurol* **375**, 467–480.
- Mulle C, Delhaye-Bouchaud N & Mariani J (1987). Peripheral maps and synapse elimination in the cerebellum of the rat. I. Representation of peripheral inputs through the climbing fiber pathway in the posterior vermis of the normal adult rat. *Brain Res* **421**, 194–210.
- Nakamura Y, Kitao Y & Okoyama S (1983). Cortico-Darkschewitsch-olivary projection in the cat: an electron microscope study with the aid of horseradish peroxidase tracing technique. *Brain Res* **274**, 140–143.
- Oka H, Jinnai K & Yamamoto T (1979). The parieto-rubro-olivary pathway in the cat. *Exp Brain Res* **37**, 115–125.
- Onodera S & Hicks TP (1995). Patterns of transmitter labelling and connectivity of the cat's nucleus of Darkschewitsch: a wheat germ agglutinin-horseradish peroxidase and immunocytochemical study at light and electron microscopical levels. *J Comp Neurol* **361**, 553–573.
- Paxinos G (2004). *The Rat Nervous System*, Third Edition. Elsevier Academic Press, Amsterdam.
- Petersen CC (2014). Cortical control of whisker movement. *Ann Rev Neurosci* **37**, 183–203.
- Provini L, Redman S & Strata P (1968). Mossy and climbing fibre organization on the anterior lobe of the cerebellum activated by forelimb and hindlimb areas of the sensorimotor cortex. *Exp Brain Res* **6**, 216–233.
- Ruigrok TJ, de Zeeuw CI, van der Burg J & Voogd J (1990). Intracellular labeling of neurons in the medial accessory olive of the cat: I. Physiology and light microscopy. *J Comp Neurol* **300**, 462–477.
- Ruigrok TJ & Teune TM (2014). Collateralization of cerebellar output to functionally distinct brainstem areas. A retrograde, non-fluorescent tracing study in the rat. *Front Syst Neurosci* **8**, 23.
- Ruigrok TJ & Voogd J (1995). Cerebellar influence on olivary excitability in the cat. *Eur J Neurosci* **7**, 679–693.
- Saint-Cyr JA (1987). Anatomical organization of cortico-mesencephalo-olivary pathways in the cat as demonstrated by axonal transport techniques. *J Comp Neurol* **257**, 39–59.
- Saint-Cyr JA & Courville J (1981). Sources of descending afferents to the inferior olive from the upper brain stem in the cat as revealed by the retrograde transport of horseradish peroxidase. *J Comp Neurol* **198**, 567–581.
- Sasaki K, Oka H, Matsuda Y, Shimono T & Mizuno N (1975). Electrophysiological studies of the projections from the parietal association area to the cerebellar cortex. *Exp Brain Res* **23**, 91–102.
- Stuesse SL & Newman DB (1990). Projections from the medial agranular cortex to brain stem visuomotor centers in rats. *Exp Brain Res* **80**, 532–544.
- Sugihara I, Marshall SP & Lang EJ (2007). Relationship of complex spike synchrony bands and climbing fiber projection determined by reference to aldolase C compartments in crus IIa of the rat cerebellar cortex. *J Comp Neurol* **501**, 13–29.
- Sugihara I & Quy PN (2007). Identification of aldolase C compartments in the mouse cerebellar cortex by olivocerebellar labeling. *J Comp Neurol* **500**, 1076–1092.
- Sugihara I & Shinoda Y (2004). Molecular, topographic, and functional organization of the cerebellar cortex: a study with combined aldolase C and olivocerebellar labeling. *J Neurosci* **24**, 8771–8785.
- Swenson RS & Castro AJ (1983). The afferent connections of the inferior olivary complex in rats. An anterograde study using autoradiographic and axonal degeneration techniques. *Neuroscience* **8**, 259–275.
- Thomson MA, Piat G, Cordonnier V, Ellouze-Kallel L, Delhaye-Bouchaud N & Mariani J (1989). Representation of vibrissae inputs through the climbing fiber pathway in lobule VII of the adult rat cerebellar vermis. *Brain Res* **488**, 241–252.
- Urbain N & Deschenes M (2007). Motor cortex gates vibrissal responses in a thalamocortical projection pathway. *Neuron* **56**, 714–725.
- Veazey RB & Severin CM (1982). Afferent projections to the deep mesencephalic nucleus in the rat. *J Comp Neurol* **204**, 134–150.

Yatim N, Billig I, Compoint C, Buisseret P & Buisseret-Delmas C (1996). Trigemino-cerebellar and trigemino-olivary projections in rats. *Neurosci Res* **25**, 267–283.

Additional information

Competing interests

All authors declare no competing financial interests.

Author contributions

R.K. and K.H. designed the study. R.K. performed experiments and analysed the data. A.A. contributed to analysis tools. R.K., A.A. and K.H. wrote the manuscript. All authors approved the final version of the manuscript and agree to be accountable for all aspects of the work in ensuring that questions related to the

accuracy or integrity of any part of the work are appropriately investigated and resolved. All persons designated as authors qualify for authorship, and all those who qualify for authorship are listed.

Funding

This work was supported by Grants-in Aid for Scientific Research (25117006, 25000015, 18H04947, 17H03551 to K.H.) from the Ministry of Education, Culture, Sports, Science and Technology of Japan and by the Strategic Research Program for Brain Sciences (17dm0107093h0002) from AMED to K.H.

Acknowledgements

We thank Ann Turnley, PhD, from Edanz Group (www.edanzediting.com/ac) for editing a draft of the manuscript.